Sigma J Eng Nat Sci, Vol. 43, No. 4, pp. 1533–1546, August, 2025

Sigma Journal of Engineering and Natural Sciences
Web page info: https://sigma.yildiz.edu.tr
DOI: 10.14744/sigma.2025.00150

Research Article

# Magnetohydrodynamic flow and effects of Soret, Dufour and thermophoresis through a chemically reacting porous stretching plate

**Ankur KUMAR SARMA[1,*], Dipak SARMA[1], Sunmoni MUDOI[1]**

[1]*Department of Mathematics, Cotton University, Pan Bazar, 781001, India*

## ARTICLE INFO

*Article history*
Received: 19 July 2024
Revised: 21 August 2024
Accepted: 03 November 2024

**Keywords:**
Magnetohydrodynamic Flow; Soret and Dufour Effects; Thermophoresis; Porous Medium

## ABSTRACT

This study investigates the novel sequel of soret, dufour, and thermophoresis on a chemically reacting porous stretching plate. With a transverse magnetic field, the fluid model is two-dimensional. Using the similarity transformation, the non-linear governing partial differential equations are converted to solvable ordinary differential equations, which are numerically solved using bvp4c. Graphs depict velocity, temperature, and concentration curves for various parameters. The values of skin friction, Nusselt number, and Sherwood number are shown in tables. The velocity profile decreases with the rise in Magnetic parameter and porosity parameter. The temperature profile escalates with the rise in thermophoretic parameter. While the concentration profile decreases with the rise in thermophoretic parameter. Also, the concentration profile escalates with the rise in Soret number. The Soret effect of a chemically reacting porous stretching plate causes species migration due to temperature gradients, whereas the Dufour effect creates heat due to concentration gradients, affecting temperature and concentration profiles. Thermophoresis moves particles over temperature gradients, impacting species distribution and reaction rates. These factors complicate heat, mass transmission, and chemical processes. In comparison with previous studies, the current results are considered to be quite excellent. Current research applies to industrial appliances, food, cosmetics, and biomedical sectors.

**Cite this article as:** Kumar Sarma A, Sarma D, Mudoi S. Magnetohydrodynamic flow and effects of Soret, Dufour and thermophoresis through a chemically reacting porous stretching plate. Sigma J Eng Nat Sci 2025;43(4):1533–1546.

## INTRODUCTION

Magnetohydrodynamics (MHD) is a field that studies the behavior of electrically conducting fluids in the presence of magnetic fields, such as plasmas, liquids, and some gases. MHD finds diverse applications across industries and scientific fields. It enables the development of innovative power generation systems, such as MHD generators that convert heat directly into electricity without moving parts, revolutionising energy production from fossil fuels, nuclear reactors, or renewable sources. MHD›s influence extends to aerospace propulsion, where it offers potential for propulsion systems in spacecraft and aircraft, leveraging the interaction between magnetic fields and conducting fluids

*Corresponding author.
*E-mail address: mth2291004_ankur@cottonuniversity.ac.in

*This paper was recommended for publication in revised form by Editor-in-Chief Ahmet Selim Dalkilic*

Published by Yıldız Technical University Press, İstanbul, Turkey

for thrust. Its role in astrophysics is pivotal, aiding in comprehending celestial phenomena like solar flares, magnetospheres, and the dynamics of cosmic plasma. MHD›s significance in fusion research involves confining and controlling high-temperature plasmas in fusion reactors through magnetic fields, contributing to advancements in clean energy production. Moreover, its applications span geophysics, industrial processes like metal casting and electromagnetic pumps, as well as fundamental research in plasma physics and fusion endeavours.

The Soret and Dufour effect are two related phenomena in fluid dynamics and heat transfer that describe the behaviour of mass and heat transfer in a fluid when there are gradients in temperature and concentration. These effects are particularly relevant in situations involving non-isothermal (temperature-varying) and non-isobaric (pressure-varying) flows. Swiss scientist Charles Soret named the thermal diffusion effect, also known as the Soret effect, in 1879, while L. Dufour introduced the diffusion thermos effect, also known as the Dufour effect, in 1873. A concentration gradient in a fluid allows molecules or particles to move owing to a temperature gradient, known as thermal diffusion or Soret effect. Comprehending the Soret effect is essential for managing the dispersion of particles and solutes in fluids, refining industrial procedures, and deciphering natural occurrences where temperature gradients impact particle behavior. In systems where accurate adjustment of concentration profiles is necessary, it is crucial. The Dufour effect, also known as thermo-diffusion, is the phenomenon where a temperature gradient in a fluid causes a change in the concentration of different components or species in the fluid. It is important to comprehend the Dufour effect in systems where mass transfer and heat transfer happen simultaneously. It makes processes more efficient and easier to control when heat and mass diffusion interact. This is done by helping engineers understand and predict how fluid mixes will behave in different situations.

The movement of particles in a fluid medium due to temperature gradients is known as thermophoresis. When there›s a variation in temperature within a fluid, it can cause particles within that fluid to migrate from regions of higher temperature to regions of lower temperature. This movement occurs due to the interaction between the particles and the temperature gradient in the surrounding medium. Various factors, including the size and properties of the particles, the temperature gradient, and the fluid characteristics, can influence the motion of particles in thermophoresis. Fields like physics, chemistry, and engineering often study it in the context of colloidal systems, where understanding the behavior of particles within a fluid has implications. In many scientific and industrial operations, managing and forecasting particle behavior requires an understanding of thermophoresis. Environmental research relies on thermophoresis as it enhances pollution dispersion models and serves engineering applications that require precise manipulation of particle distributions. Thermophoresis has applications in a variety of fields, including the manipulation of particles in microfluidic devices, the study of aerosols and particle transport, and the development of certain materials and coatings. This phenomenon allows for improved heat management by changing fluid characteristics and thermal boundary layers, which is critical for streamlining industrial operations. It manipulates particle trajectories by interacting with magnetic fields to regulate particle deposition and migration, which is essential in applications like coatings and pollution management. Thermophoresis also changes the structure and stability of the flow, which makes it possible to precisely control how the fluid acts in MHD-driven systems and improves their usefulness in areas such as electromagnetic pumping and plasma processing.

Cortell [1], Ibrahim [2], and Shateyi [3] disregarded the outcomes of the Soret and Dufour effects in heat and concentration transport, citing variations in the consequences reported by the Fick›s and Fourier laws. Eckert and Drake [4] noted that the Soret effect affects isotope separation and the combination of low (He, H2) and medium molecular weight gases (H2, air). Afterwards, many researchers, including Sattar and Alam [5], extensively studied their significance in heat transfer problems. Chamkha and Rashad [6] investigated the Soret and Dufour effect on mixed convection flow around a vertical cone with an angular velocity. Mortimer and Eyring [7] used simple transition states to construct the Soret and Dufour phenomenon. Tak, Khan, and Mathur [8] studied double diffusion inside a Darcy porous media on a vertical permeable surface. The Soret and Dufour impact on MHD mixed convection over an infinite vertical porous plate was analyzed by Ahmed and Sengupta [9]. In porous media, Moorthy and Senthilvadivu [10] quantitatively studied the Soret and Dufour impact on MHD-free convection with varied velocities Reddy and Chamkha [11] solved the Soret and Dufour effects of MHD convective flow across a stretched sheet in porous media numerically. Jha and Gambo [12] presented their investigation of the sequel to Soret and Dufour on unsteady free convection, where the bounding wall has ramped temperature and the species has ramped concentration, respectively. Ashraf, Hayat, Alsaedi, and Shehzad [13] investigated Soret and Dufour›s effects on an Oldroyd-B fluid in the presence of convective boundary conditions. They used the homotopy analysis method to describe this phenomenon. Gbadeyan, Idowu, Ogunsola, Agboola, and Olanrewaju [14] studied the Soret and Dufour effects on mixed convection heat and mass transfer flow over a stretching surface filled with viscoelastic fluid. They compared the Runge-Kutta shooting technique with the Ham method for the zero magnetic field parameter. Srinivasacharya and RamReddy [15] studied thermo-diffusion and diffusion-thermo on an exponentially stretched surface using a quiescent fluid. Siddique, Nadeem, Awrejcewicz, and Pawtowski [16] examined Soret and Dufour on an unstable MHD second-grade nanofluid over an exponential surface. Another

work by Mahdy, A. [17], used a different boundary layer of non-Darcian mixed convective flow to show what happens when there is suction and injection along with double diffusion. Srinivasacharya and RamReddy [18] researched the cross diffusion effect on an exponentially extended sheet in a non-Darcy quiescent fluid using the Keller Box method. In MHD mixed convection heat and mass transfer flow with radiation, hall current, Soret, and Dufour, Shateyi et al. [19] described the magnetic field›s effect. Shaheen et al. [20] examined the sequel of Soret and Dufour to a 2D Casson nanofluid in a deformable cylinder. The variables they used were the Arrhenius activation energy and chemical reaction. Considering Hall current and heat flux, Quader and Alam [21] used the FDM technique to show the double diffusion effect on unsteady natural convection. Subhakar, Gangadhar, and Reddy [22] used a moving, non-isothermal vertical plate to understand the influence of Soret and Dufour on heat generated or absorbed. Balla et al. [23] used Hillesdon and Pedley›s model to demonstrate nanofluid bioconvective flow and further inquired about the sequel of Soret and Dufour on it. Reddy, Rao, and Vijaya [24] considered a viscoelastic fluid to show the Soret and Dufour effect passing through an infinitely extended sheet. Rashed [25] worked on the thermophoresis effect, variable velocity in non-Darcian flow, the occurrence of Soret, Dufour, and thermal radiation. A number of researchers [26–40, 41–65] have recently focused on the investigation of diverse impacts, such as thermophoresis and magnetic fields, on various fluid flow characteristics and geometry.

We have expanded upon the work of Ishak [66] to address unsteady MHD forced convection over a stretching plate. We apply the Soret, Dufour, thermophoresis, and chemical reaction sequel to our work, focusing on a 2D steady flow. To the author›s knowledge, no one has yet examined the combined effects of thermophoresis, Dufour, chemical reaction, soret, and joule heating on a continuous MHD flow through a porous stretched plate. The examination of all these combined impacts in fluid flow was the main focus of this investigation. Also, when compared to previous studies, the new results are considered to be quite good.

## MATHEMATICAL FORMULATION

We consider a 2D coordinate system. The surface is extended along the x-axis with velocity $U_W = ax$, keeping the origin stationary. The transverse magnetic field $M_0$ is applied externally $90^0$ to x-axis in positive direction of y-axis. The y-axis is considered normal to stretching plate, while x-axis is parallel to stretching plate. The flow problem is graphically demonstrated in Figure 1, where $u$ and $v$ are the velocity of the fluid along x and y direction respectively. In the course of our analysis, we have taken into consideration the following assumptions on the flow problem:

- Fluid is contained in a porous media and is thought to be electrically conducting with electrical conductivity ($\sigma_e$).

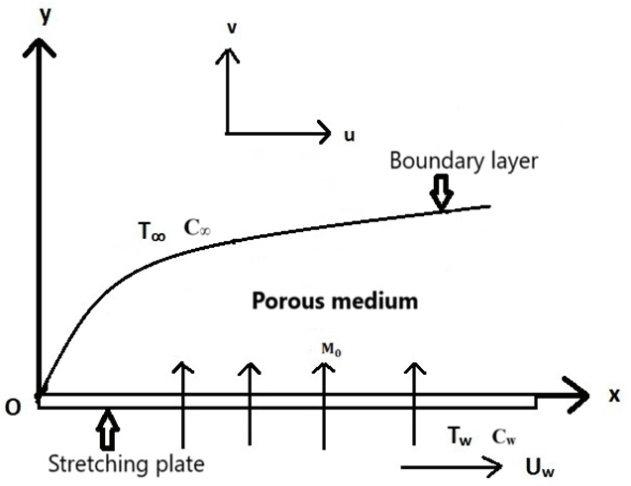


**Figure 1.** Geometry of the flow problem.

- Magnetic field induced is neglected and the magnetic Reynolds is considered to be small.
- Fluid is considered to be steady, 2D, laminar and incompressible.
- Fluid is taken to be chemically reacting with a first order chemical reaction.
- The flow issue assumes no external electric field.
- Hall effect and polarisation of charges are neglected.

These assumptions with Boussinesq's approximation provide the continuity, momentum, energy, and concentration equations [6]:

Continuity equation:

$$\frac{\partial u}{\partial x} = -\frac{\partial v}{\partial y} \tag{1}$$

Momentum equation:

$$u\frac{\partial u}{\partial x} + v\frac{\partial u}{\partial y} = \nu\frac{\partial^2 u}{\partial y^2} - \frac{\sigma_e M_0^2 u}{\rho} - \frac{\nu u}{k_0} \tag{2}$$

Energy equation:

$$u\frac{\partial T}{\partial x} + v\frac{\partial T}{\partial y} = \alpha\frac{\partial^2 T}{\partial y^2} + \frac{\sigma_e M_0^2 u^2}{\rho C_p} + \frac{D_M K_T}{C_s C_p}\frac{\partial^2 C}{\partial y^2} \tag{3}$$

Concentration equation:

$$u\frac{\partial C}{\partial x} + v\frac{\partial C}{\partial y} = D_M\frac{\partial^2 C}{\partial y^2} - K^*(C - C_\infty) + \frac{D_M K_T}{T_M}\frac{\partial^2 T}{\partial y^2} - \frac{\partial}{\partial y}\left(V_t(C - C_\infty)\right) \tag{4}$$

where, $V_t = \frac{\nu K_T}{T_r}\frac{\partial T}{\partial y}$ is the thermophoretic velocity.

The relevant BCs [66] are:

$$y = 0: \quad u = U_w, \quad v = 0, \quad T = T_w, \quad C = C_w, \text{ and} \tag{5}$$

$$y \to \infty: \quad u \to 0, \quad T \to T_\infty, \quad C \to C_\infty \tag{6}$$

It is determined that the boundary conditions are selected in such a manner that, initially close to the plate at $y = 0$, $u = U_W$, which is the extended velocity of the surface, $v = 0$, is seeked. However, the temperature and concentration of the fluid are considered at the surface, which are denoted by the symbols $T_w$ and $C_w$ accordingly. Also, far from plate at $y \to \infty$, $u \to 0$, and the temperature and concentration of the fluid are considered to be the ambient temperature and concentration, which are denoted by the symbols $T_\infty$ and $C_\infty$ accordingly.

We consider:

$$T_w = T_\infty + bx, \quad C_w = C_\infty + dx \tag{7}$$

The continuity equation (1) is fulfilled, by using a stream function ψ such that $\mathrm{u} = \frac{\partial \psi}{\partial \mathrm{y}}$ and $\mathrm{v} = -\frac{\partial \psi}{\partial \mathrm{x}}$.

Using similarity variables and nondimensional values, the nonlinear PDEqs (2)-(4) are turned into nonlinear ODEqs:

$$\eta = \left(\frac{a}{\nu}\right)^{\frac{1}{2}} y, \quad \psi = (av x^2)^{\frac{1}{2}} f(\eta), \; \theta(\eta) = \frac{T - T_\infty}{T_w - T_\infty},$$

$$M = \frac{\sigma_e M_0^2}{\rho a}, \quad S_p = \frac{\nu}{k_0 a}, \quad Ec = \frac{a^2 x}{b C_p}, \quad \alpha = \frac{\kappa}{\rho C_p}, \quad K = \frac{K^*}{a},$$

$$\zeta = \frac{K_T (T_w - T_\infty)}{T_r} \quad Pr = \frac{\mu C_p}{\kappa}, \quad Sc = \frac{\nu}{D_M},$$

$$Du = \frac{D_M K_T (C_w - C_\infty)}{\nu C_s C_p (T_w - T_\infty)}, \quad Sr = \frac{D_M K_T (T_w - T_\infty)}{\nu T_M (C_w - C_\infty)}$$

The transformed nonlinear ODEs are:

$$f''' + ff'' - f'^2 - Mf' - S_p f' = 0 \tag{8}$$

$$\theta'' + PrMEcf'^2 + PrDu\phi'' + Pr(f\theta' - \theta f') = 0 \tag{9}$$

$$\phi'' - ScK\phi + ScSr\theta'' + Sc(f\phi' - \phi f') - Sc\zeta(\phi'\theta' + \phi\theta'') = 0 \tag{10}$$

Also, transformed beginning and boundary conditions:

$$f(0) = 0, \quad f'(0) = 1, \quad \theta(0) = 1, \quad \phi(0) = 1 \text{ and}$$
$$f'(\infty) \to 0, \quad \theta(\infty) \to 0, \quad \phi(\infty) \to 0 \tag{11}$$

The coefficient of skin friction, Nusselt and Sherwood number are as follows:

$$Re_x^{\frac{1}{2}} C_f = f''(0), \; Re_x^{-\frac{1}{2}} Nu_x = -\theta'(0) \text{ and } Re_x^{-\frac{1}{2}} Sh_x = -\phi'(0) \tag{12}$$

**Method of Solution**

Solution in MATLAB bvp4c analyses linear or nonlinear boundary value issues. It can forecast y(x) for each x in [a,b] while accounting for BCs at each step. BCs at infinity are adjusted for individuals who can logically address the present problem using this technique. By applying this method, the BCs at ∞ are adjusted to a position where solving the present issue becomes feasible. The three-stage Lobatto IIIa formula is a finite difference code in Bvp4c. Shampine et al. recommended Lobato IIIa [67]. This collocation polynomial gives uniform fourth-order accurate solutions across the interval by partitioning it into subintervals with a mesh of points. The solver calculates numerical error for each subinterval. If the answer fails tolerance, the mesh is adjusted and the procedure repeated. In addition to the original mesh points, a grid point solution assumption is always needed. An initial estimate at the beginning mesh points and step size adjustments attain the necessary accuracy. To use the finite difference based solution bvp4c, the equations (8), (9), and (10) are changed as follows.

$$f = y_1, f' = y_1' = y_2, f'' = y_2' = y_3, \theta = y_4, \theta' = y_4' = y_5,$$
$$\phi = y_6, \phi' = y_6' = y_7, \; y_3' = -y_1 y_3 + y_2^2 + M y_2 + S_p y_2 \tag{13}$$

$$y_5' = Pr[-MEcy_2^2 - Duy_7' - (y_1 y_5 - y_4 y_2)] \tag{14}$$

$$y_7' = Sc[Ky_6 - Sry_5' - (y_1 y_7 - y_6 y_2) + \zeta(y_7 y_5 + y_6 y_5')] \tag{15}$$

Also, the BCs (11) are changed accordingly

$$y_1(0) = 0, \quad y_2(0) = 1, \quad y_4(0) = 1, \quad y_6(0) = 1 \tag{16}$$

$$y_2(\infty) = 0, \quad y_4(\infty) = 0, \quad y_6(\infty) = 0 \tag{17}$$

The MATLAB solver bvp4c uses the above modified results to do the numerical computation. To fulfil convergence criteria, precision is tested to the sixth decimal point. This approach was explained in depth by Shampine *et al.* [67]. This scheme's algorithm is shown in Fig. 2 [68].

**Validation**

When comparing the current equations with the equations described by Ishak [66], the values of −θ'(0) for various values of Pr show good agreement with the present results. It is likely that the bvp4c technique will be used to compare the results for −θ'(0), disregarding the other parametric values for different values of Pr as shown in Table 1.

**Table 1.** Comparison of −θ'(0) for several values of Pr

| Pr | Ishak [66] | Present values | Error |
|---|---|---|---|
| 1 | 0.9548 | 0.9548 | 0.0000 |
| 2 | 1.4715 | 1.4715 | 0.0000 |
| 3 | 1.8691 | 1.8691 | 0.0000 |

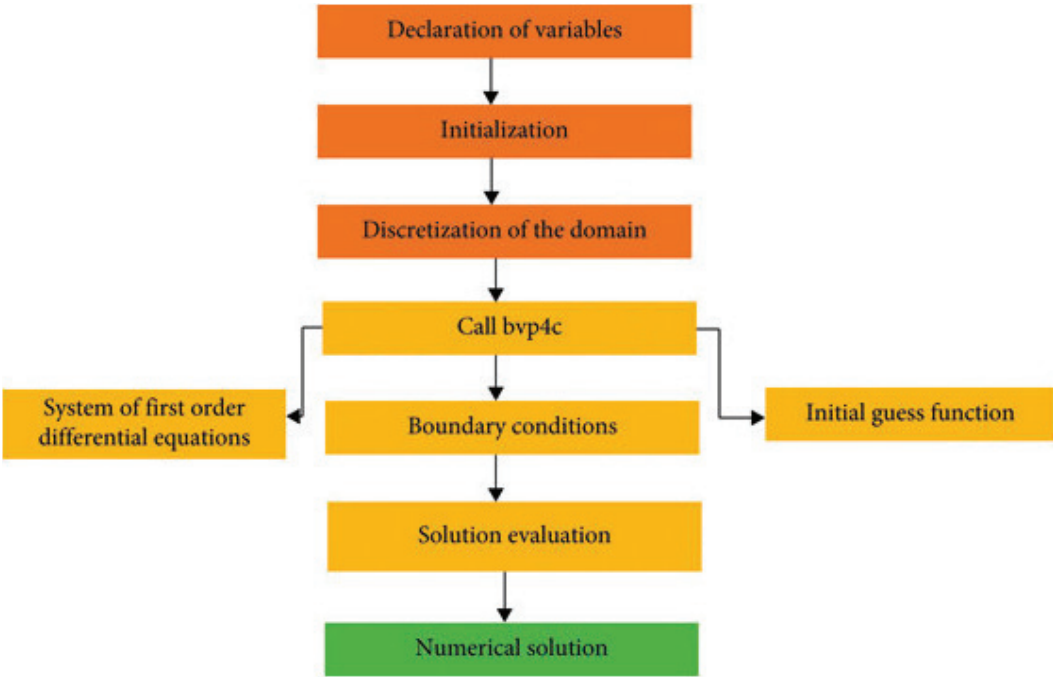


**Figure 2.** bvp4c algorithm.

## RESULTS AND DISCUSSION

Numerical computations for the problem parameters are presented graphically from Figure 3 to 13. Also, the variation of the skin friction, Nusselt and Sherwood number are displayed via Tables 2 to 6. The standard values of the parameters are taken as Pr = 0.7 (air), $Ec$=0.05, $M$=0.4, $S_p$=0.4, $Sc$=0.4, $Sr$=0.4, $Du$=0.4, $K$=1 recognised by Ishak [66], Elbashbeshy *et al.* [69]. Additionally, M is chosen to be minimal because generated magnetic field, Hall current, and ion slip are all factors that contribute to the magnetic field›s perceived weakness.

Figure 3 demonstrates that the velocity profile declines as M (Hartman number) rises. This is due to the effect of Lorentz force, which detards the motion of fluid flow. This phenomenon affects magnetohydrodynamics (MHD) applications, such as nuclear reactor cooling systems, where the magnetic field controls fluid flow. In electromagnetic pumps and fusion reactor plasma confinement, the magnetic field regulates ionised fluid flow. Figure 4 illustrates the sequel of $S_p$ on the flow profile. It shows that as $S_p$ escalates, the fluid flow declines. This is due to the fact, as the occurrence of porous medium causes resistance to the fluid flow and as a result the flow profile reduces. Controlling flow via porous structures is important in oil recovery, groundwater filtering, and bioengineering. For improved oil recovery, adjusting porosity may affect reservoir fluid extraction. In groundwater filtration, water flow is controlled via soil or filters. Figure 5 shows the impact of M on the temperature profile. As M escalates, the fluid's temperature rises. Owing to the fact that as the magnetic field rises the fluid particles starts vibrating frequently as such increasing the fluid's temperature. Figure 6 illustrates the impact of Du on the temperature profile. As Du escalates, the fluid's temperature rises. Higher Du values enhance boundary layer thickness and fluid temperature, resulting in fast energy transfer. Figure 7 displays the impact of Eckert number on temperature. The fluid›s temperature escalates as Ec increases, indicating a decrease in enthalpy and rise in kinetic energy. Viscous dissipation converts kinetic energy into heat, raising fluid temperature as Eckert number increases. For performance, efficiency, and safety, temperature management is crucial in high-speed flow systems including aerospace vehicles, turbomachinery, microfluidics, biomedical devices, and industrial operations like polymer extrusion and lubrication. Figure 8 depicts the temperature curve and the sequel of Pr. When Pr increases, temperature decreases, demonstrating a link between velocity and thermal boundary layer thickness. Escalating values of Pr are thought to imply that thermal diffusivity is dominating, and hence the thermal boundary layer is thinner than the velocity boundary layer. From Figure 9 it is seen that as $\zeta$ (thermophoretic parameter) escalates, the fluid's temperature rises. Owing to the fact that, as increase in $\zeta$ means that particles are more responsive to the temperature gradient. This leads to enhanced movement of particles from hot to cold regions. Evidently, fluid's temperature escalates. As the thermophoretic parameter increases, particles move away from hot locations, reducing heat loss. This raises local temperatures, which helps with combustion, material processing, and industrial furnace activities that require focused heat,

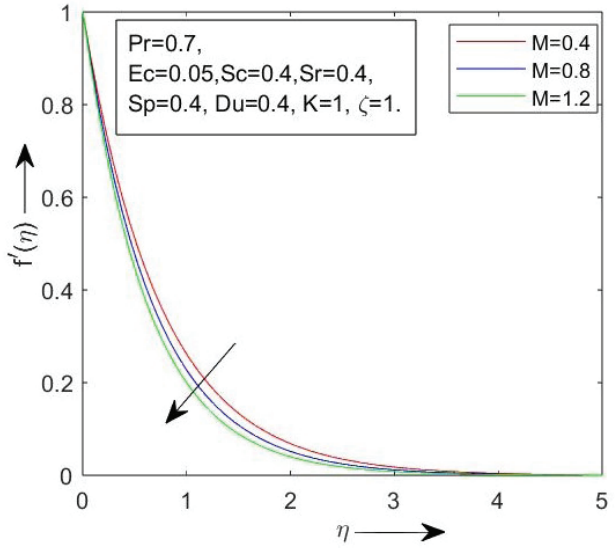


**Figure 3.** Velocity profile vs M.

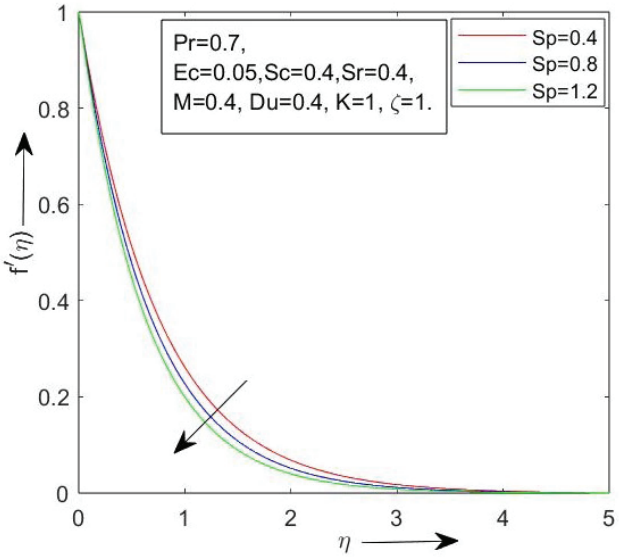


**Figure 4.** Velocity profile vs $S_p$.

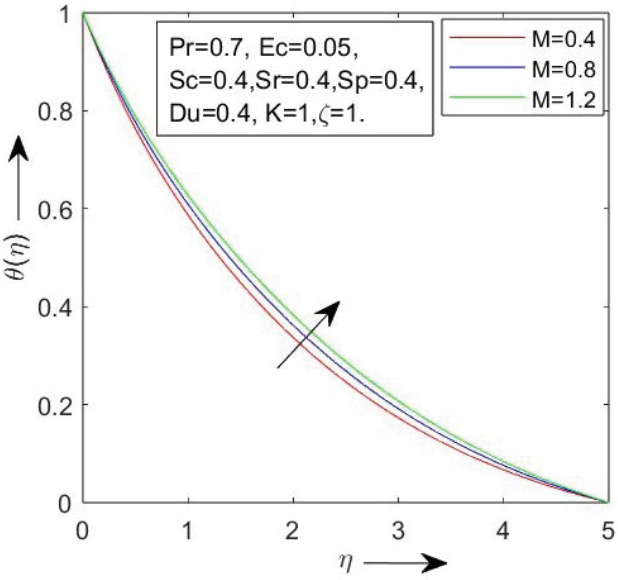


**Figure 5.** Heat profile vs M.

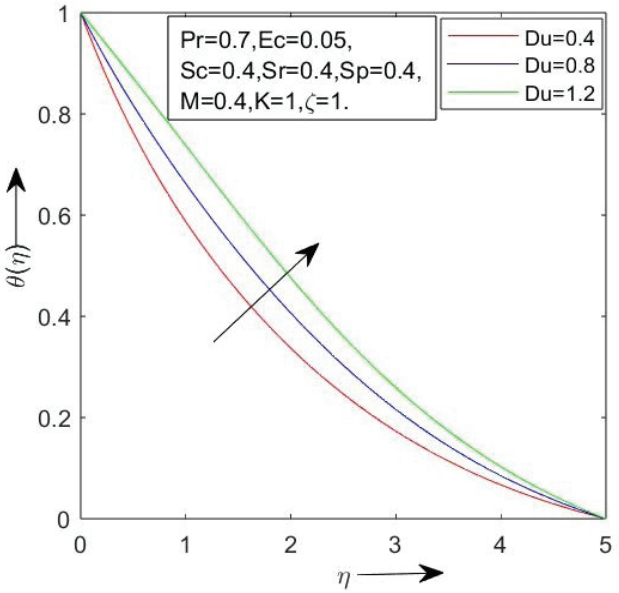


**Figure 6.** Heat profile vs Du.

thermal insulation, or heat transmission. The impact of K causes a considerable decrease in fluid concentration, as seen in Figure 10. The concentration of the fluid falls as K rises because it represents the reaction rate, or the speed at which reactants turn into products. Reactants are consumed more quickly at a higher reaction rate, which lowers the concentration of reactants in the fluid. If the products do not refill the reactants or if the reactants are not continually supplied, then this increased consumption lowers the overall concentration of the reacting species. Fluid concentration gradually decreases as a result of the quicker depletion of reactant concentration brought on by the faster chemical processes. This is consistent with the physical fact that species consumption leads to a decrease in species concentration. From, Figure 11 illustrates that as Sc escalates, the fluid's concentration decreases. It is due to the fact that as Sc rises, it rises the fluid's viscosity and hence decreasing fluid's concentration. As the Schmidt number increases, momentum diffusivity takes precedence over mass diffusivity. The fluid›s solutes and particles diffuse more slowly than its viscous diffusion. An increased Schmidt number reduces diffusing species concentration, altering chemical mixing, pollution management, and heat transfer systems. Figure 12 shows that for superior

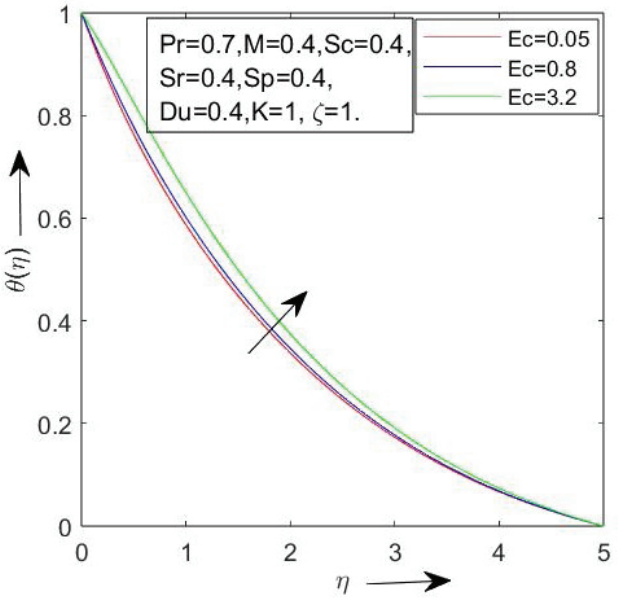


**Figure 7.** Heat profile vs Ec.

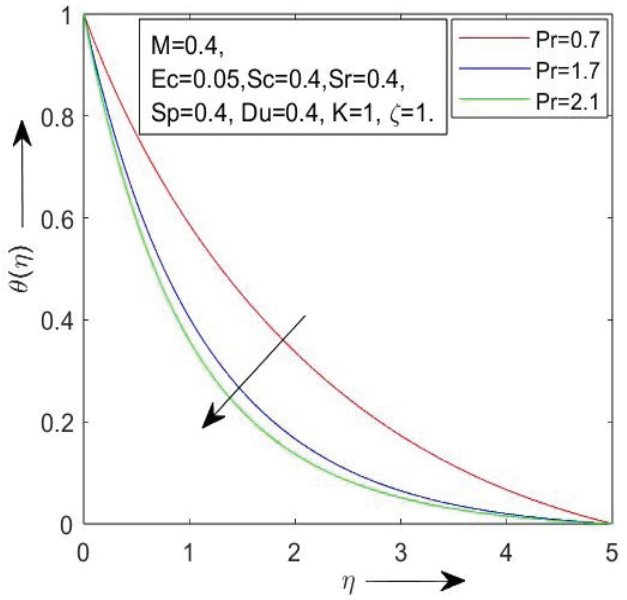


**Figure 8.** Heat profile vs Pr.

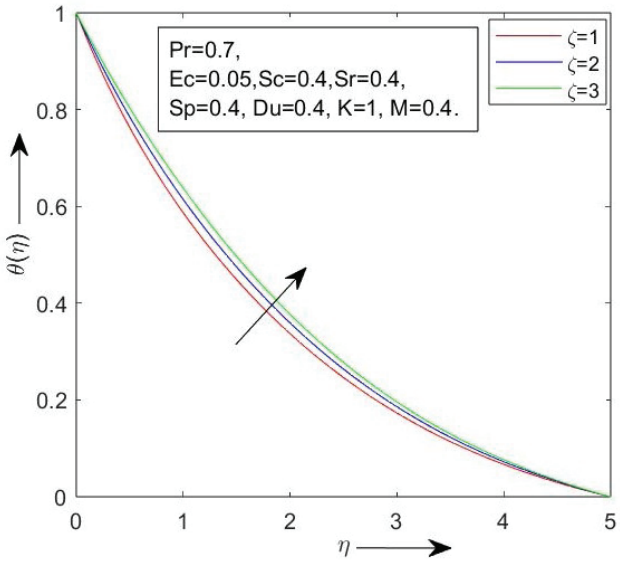


**Figure 9.** Heat profile vs ζ.

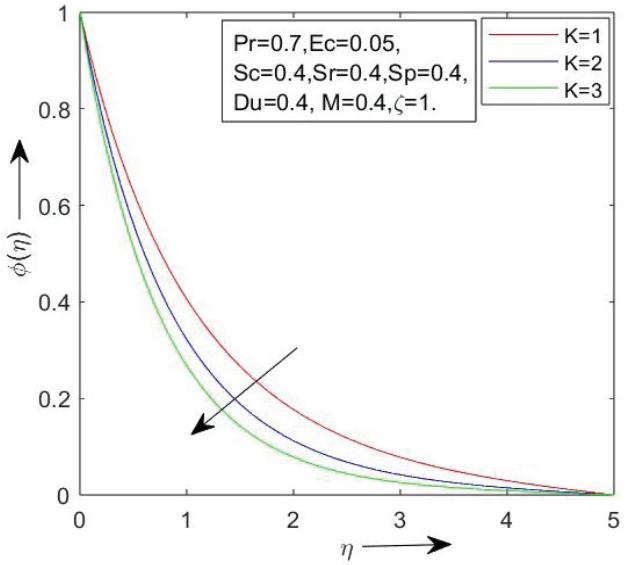


**Figure 10.** Concentration profile vs K.

values of Sr, the concentration profile escalates. Greater Soret numbers correlate to greater temperature gradients, which in turn produce more convective flow. The fluid›s concentration escalates with a hike in the Soret number because this number quantifies the effect of thermal diffusion, where a temperature gradient induces a concentration gradient. A greater Soret number implies better thermodiffusion, which moves particles or solutes from low to high temperatures. Because of migration, solutes accumulate in some places, increasing their concentration. Essentially, the Soret effect redistributes the solutes more effectively with a higher Soret number, enhancing the local concentration where the temperature gradient drives the solutes to accumulate. Hence, concentration distribution escalates. From Figure 13 it is seen that as ζ escalates, fluid's concentration declines. The thermophoretic parameter, which quantifies how well particles move in response to a temperature gradient, decreases as the value rises. Particles move from hot to cold areas faster as it rises, creating a net outflow from areas with higher concentrations. Although the distribution becomes more even as a result of this shift, the concentration in the formerly higher-density areas

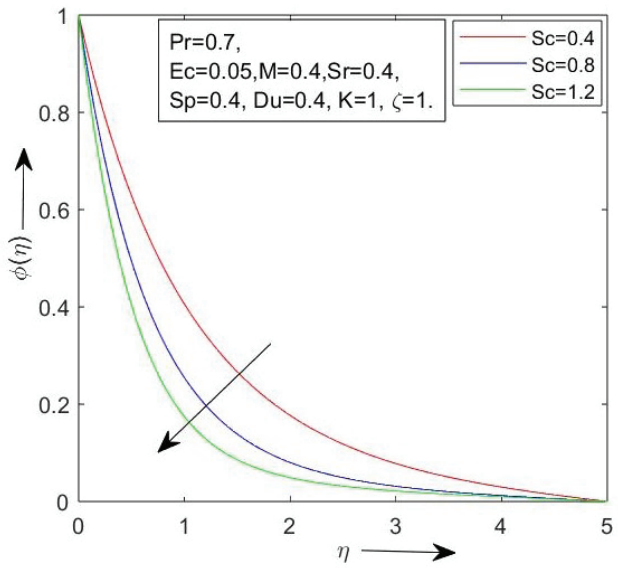


**Figure 11.** Concentration profile vs Sc.

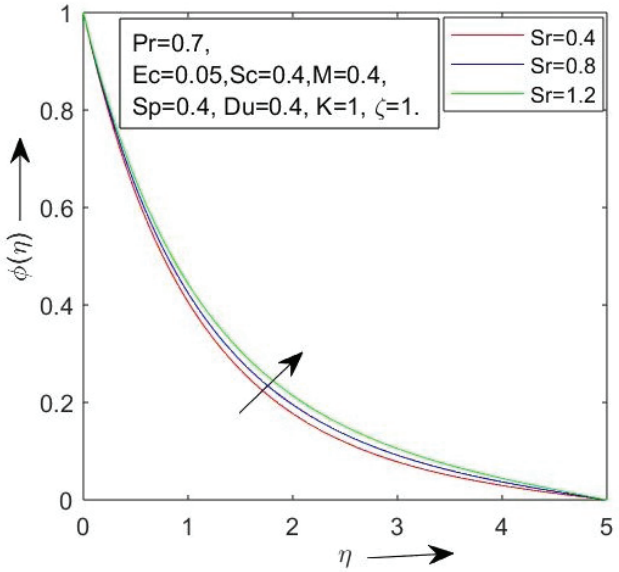


**Figure 12.** Concentration profile vs Sr.

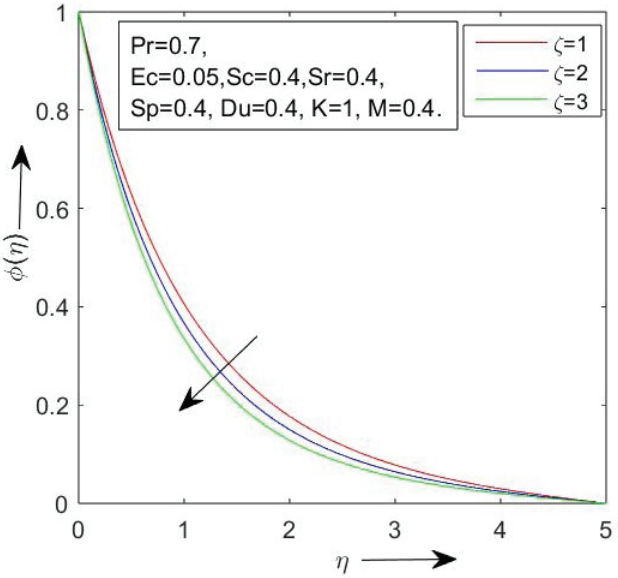


**Figure 13.** Concentration profile vs ζ.

decreases. The enhanced thermophoretic effect dilutes local concentrations, particularly in close proximity to heat sources, leading to a general decrease in the solute or particle concentration in the fluid as they disperse more evenly. A higher thermophoretic parameter increases particle movement in response to temperature gradients, lowering concentration in hotter locations. This idea applies to particle movement and deposition in pollution control, manufacturing, cooling systems, and biological applications.

The variation in the skin friction coefficient, Nusselt and Sherwood number are shown in Tables 2 to 6. From Table 2, it can be noticed that the magnitude of skin friction escalates with the upsurge in M and $S_p$. From Table 3, it is noticed that magnitude of Nusselt number (i.e., the rate of heat transfer) escalates with the upsurge in Pr, whereas it decreases with upsurge in M, $S_p$ and Ec. From Table 4, We can observe that the rate of heat transfer decreases with the upsurge in Sc, Du, K and ζ, whereas it increases with the rise in Sr. From Table 5, it can be seen that the magnitude of Sherwood number decreases with the rise in M, $S_p$ and Ec,

**Table 2.** Skin friction with the variation of M and $S_p$.

| Pr | M | $S_p$ | Ec | Sc | Du | Sr | K | −f"(0) |
|---|---|---|---|---|---|---|---|---|
| 0.7 | 0.4 | 0.4 | 0.05 | 0.4 | 0.4 | 0.4 | 1 | -1.3417 |
| | 0.8 | | | | | | | -1.4833 |
| | 1.2 | | | | | | | -1.6125 |
| 0.7 | 0.4 | 0.4 | 0.05 | 0.4 | 0.4 | 0.4 | 1 | -1.3417 |
| | | 0.8 | | | | | | -1.4833 |
| | | 1.2 | | | | | | -1.6125 |

**Table 3.** Nusselt number with the variation of Pr, M, $S_p$ and Ec

| Pr | M | $S_p$ | Ec | Sc | Du | Sr | K | $-\theta'(0)$ |
|---|---|---|---|---|---|---|---|---|
| 0.7 | 0.4 | 0.4 | 0.05 | 0.4 | 0.4 | 0.4 | 1 | 0.5633 |
| 1.0 | | | | | | | | 0.6926 |
| 1.7 | | | | | | | | 0.9398 |
| 0.7 | 0.4 | 0.4 | 0.05 | 0.4 | 0.4 | 0.4 | 1 | 0.5633 |
| | 0.8 | | | | | | | 0.5315 |
| | 1.2 | | | | | | | 0.5046 |
| 0.7 | 0.4 | 0.4 | 0.05 | 0.4 | 0.4 | 0.4 | 1 | 0.5633 |
| | | 0.8 | | | | | | 0.5354 |
| | | 1.2 | | | | | | 0.5118 |
| 0.7 | 0.4 | 0.4 | 0.05 | 0.4 | 0.4 | 0.4 | 1 | 0.5633 |
| | | | 1.50 | | | | | 0.4416 |
| | | | 2.50 | | | | | 0.3576 |

**Table 4.** Nusselt number variation w.r.t. Sc, Du, Sr, K and $\zeta$.

| Pr | M | $S_p$ | Ec | Sc | Du | Sr | K | $\zeta$ | $-\theta'(0)$ |
|---|---|---|---|---|---|---|---|---|---|
| 0.7 | 0.4 | 0.4 | 0.05 | 0.4 | 0.4 | 0.4 | 1 | 1 | 0.5633 |
| | | | | 0.8 | | | | | 0.4794 |
| | | | | 1.2 | | | | | 0.4195 |
| 0.7 | 0.4 | 0.4 | 0.05 | 0.4 | 0.4 | 0.4 | 1 | 1 | 0.5633 |
| | | | | | 0.8 | | | | 0.4084 |
| | | | | | 1.2 | | | | 0.2587 |
| 0.7 | 0.4 | 0.4 | 0.05 | 0.4 | 0.4 | 0.4 | 1 | 1 | 0.5633 |
| | | | | | | 0.8 | | | 0.5731 |
| | | | | | | 1.2 | | | 0.5835 |
| 0.7 | 0.4 | 0.4 | 0.05 | 0.4 | 0.4 | 0.4 | 1 | 1 | 0.5633 |
| | | | | | | | 2 | | 0.5147 |
| | | | | | | | 3 | | 0.4679 |
| 0.7 | 0.4 | 0.4 | 0.05 | 0.4 | 0.4 | 0.4 | 1 | 1 | 0.5633 |
| | | | | | | | | 2 | 0.4931 |
| | | | | | | | | 3 | 0.4331 |

**Table 5.** Sherwood number with the variation of Pr, M, $S_p$ and Ec

| Pr | M | $S_p$ | Ec | Sc | Du | Sr | K | $-\phi'(0)$ |
|---|---|---|---|---|---|---|---|---|
| 0.7 | 0.4 | 0.4 | 0.05 | 0.4 | 0.4 | 0.4 | 1 | 0.9689 |
| 1.0 | | | | | | | | 0.9936 |
| 1.7 | | | | | | | | 1.0418 |
| 0.7 | 0.4 | 0.4 | 0.05 | 0.4 | 0.4 | 0.4 | 1 | 0.9689 |
| | 0.8 | | | | | | | 0.9528 |
| | 1.2 | | | | | | | 0.9393 |
| 0.7 | 0.4 | 0.4 | 0.05 | 0.4 | 0.4 | 0.4 | 1 | 0.9689 |
| | | 0.8 | | | | | | 0.9537 |
| | | 1.2 | | | | | | 0.9408 |
| 0.7 | 0.4 | 0.4 | 0.05 | 0.4 | 0.4 | 0.4 | 1 | 0.9689 |
| | | | 1.50 | | | | | 0.9435 |
| | | | 2.50 | | | | | 0.9261 |

**Table 6.** Sherwood number with the variation of Sc, Du, Sr, K and ζ

| Pr | M | $S_p$ | Ec | Sc | Du | Sr | K | ζ | $-\phi'(0)$ |
|---|---|---|---|---|---|---|---|---|---|
| 0.7 | 0.4 | 0.4 | 0.05 | 0.4 | 0.4 | 0.4 | 1 | 1 | 0.9689 |
| | | | | 0.8 | | | | | 1.4529 |
| | | | | 1.2 | | | | | 1.8345 |
| 0.7 | 0.4 | 0.4 | 0.05 | 0.4 | 0.4 | 0.4 | 1 | 1 | 0.9689 |
| | | | | | 0.8 | | | | 0.9390 |
| | | | | | 1.2 | | | | 0.9105 |
| 0.7 | 0.4 | 0.4 | 0.05 | 0.4 | 0.4 | 0.4 | 1 | 1 | 0.9689 |
| | | | | | | 0.8 | | | 0.9273 |
| | | | | | | 1.2 | | | 0.8832 |
| 0.7 | 0.4 | 0.4 | 0.05 | 0.4 | 0.4 | 0.4 | 1 | 1 | 0.9689 |
| | | | | | | | 2 | | 1.1825 |
| | | | | | | | 3 | | 1.3544 |
| 0.7 | 0.4 | 0.4 | 0.05 | 0.4 | 0.4 | 0.4 | 1 | 1 | 0.9689 |
| | | | | | | | | 2 | 1.0915 |
| | | | | | | | | 3 | 1.1807 |

whereas it escalates with the rise in Pr. From Table 6, it can be observed that magnitude of Sherwood number escalates with the rise in Sc, K and ζ, whereas it decreases with the rise in Du and Sr.

## CONCLUSION

The novel aspect of the current research is to study the sequel of Soret, Dufour and thermophoresis in a chemically reacting stretching porous plate in occurrence of a transverse magnetic field. The following results can be concluded from the above study:

- The flow profile decreases with the rise of M and $S_p$.
- The heat profile escalates with the rise of M, Du, Ec and ζ. While it decreases with the rise of Pr.
- Concentration profile decreases with the rise of K, Sc and ζ, whereas it escalates with the rise in Sr.
- Magnitude of skin friction coefficient escalates with the rise in M and $S_p$.
- Magnitude of heat transfer rate upsurges with the rise in Pr and Sr, whereas it decreases with the rise in M, $S_p$, Ec, Sc, Du, K and ζ.
- The magnitude of mass transfer rate upsurges with the rise in Pr, Sc, K and ζ, whereas it decreases with the rise in M, $S_p$, Ec, Du and Sr.

The current investigation should primarily focus on future work on the irregular behavior of the problem and its relevance to entropy production and activation energy. Significant sequel of thermal radiation, heat source, thermophoresis, and chemical reaction parameters on flow profiles can be found in a broad range of industrial and technological applications, including metallic coating, crystal growth, electromagnetic pumps, power generators, MHD accelerators, and reactor cooling. The study›s conclusions might be used to a variety of processes, including paper manufacture, suspensions, heat exchanger technology, material processing, drying, and surface evaporation of water bodies. It is also possible to expand this work to a three-dimensional flow issue and investigate the varied flow effects for non-Newtonian fluids, including Maxwell, Carreau, and Williamson fluids.

## NOMENCLATURE

| | |
|---|---|
| a,b,d | Constant, |
| $M_0$ | Constant Magnetic field, (Nm/A) |
| $C_p$ | Specific heat at constant pressure, $(\frac{J}{kgK})$ |
| $C_s$ | Concentration susceptibility, |
| $K^*$ | Rate of first order chemical reaction, |
| f | Dimensionless stream function, |
| Ec | Eckert number, |
| $k_0$ | Permeability of porous medium, $(m^2)$ |
| M | Magnetic parameter (Hartmann number), |
| Pr | Prandlt number, |
| $S_p$ | Porosity parameter, |
| ζ | Thermophoretic parameter, |
| $D_M$ | Coefficient of molecular diffusivity, |
| $D_T$ | Coefficient of thermal diffusivity, |
| $K_T$ | Thermal diffusion ratio, |
| $T_r$ | Reference temperature, (K) |
| $T_M$ | Mean fluid temperature, |
| Sc | Schmidt number, |
| Sr | Soret number, |
| Du | Dufour number, |
| K | Chemical reaction parameter, |
| T | Fluid›s temperature, (K) |
| C | Species concentration, $(kg/m^3)$ |
| u | fluid›s velocity through x-axis, (m/s) |
| v | fluid›s velocity through y-axis, (m/s) |
| (x,y) | Cartesian coordinates |

**Greek Symbols**

| | |
|---|---|
| ρ | fluid's density, (kg/m$^3$) |
| μ | fluid›s viscosity, (Pa s) |
| σe | Electrical conductivity, ($\frac{1}{\Omega m}$) |
| η | Dimensionless similarity variable, |
| $\kappa$ | Thermal conductivity, ($\frac{W}{mK}$) |
| $\nu$ | Kinematic viscosity, (m$^2$/s) |
| $\alpha$ | Thermal diffusivity, (m$^2$/s) |
| ψ | Stream function, |
| θ | Dimensionless temperature, |

**Superscript**

| | |
|---|---|
| ' | Derivative w.r.t η |

**Subscript**

| | |
|---|---|
| w | Properties at the plate |
| ∞ | Free stream condition |

**Abbrebiation**

| | |
|---|---|
| MHD | Magnetohydrodynamics |
| ODE | Ordinary differential equation |
| PDE | Partial differential equation |
| BC | Boundary Conditions |
| 2D | Two-Dimensional |

## AUTHORSHIP CONTRIBUTIONS

Authors equally contributed to this work.

## DATA AVAILABILITY STATEMENT

The authors confirm that the data that supports the findings of this study are available within the article. Raw data that support the finding of this study are available from the corresponding author, upon reasonable request.

## CONFLICT OF INTEREST

The author declared no potential conflicts of interest with respect to the research, authorship, and/or publication of this article.

## ETHICS

There are no ethical issues with the publication of this manuscript.

## STATEMENT ON THE USE OF ARTIFICIAL INTELLIGENCE

Artificial intelligence was not used in the preparation of the article.

## REFERENCES


[1] Cortell R. Suction, viscous dissipation and thermal radiation effects on the flow and heat transfer of a power-law fluid past an infinite porous plate. Chem Eng Res Des 2011;89:85–93. [CrossRef]

[2] Ibrahim FS, Elaiw AM, Bakr AA. Effect of the chemical reaction and radiation absorption on the unsteady MHD free convection flow past a semi-infinite vertical permeable moving plate with heat source and suction. Commun Nonlinear Sci Numer Simul 2008;13:1056–1066. [CrossRef]

[3] Shateyi S. Thermal radiation and buoyancy effects on heat and mass transfer over a semi-infinite stretching surface with suction and blowing. J Appl Math 2008;2008:1–12. [CrossRef]

[4] Eckert ERG, Drake RM. Analysis of heat and mass transfer, Jr. McGraw-Hill; 1972. AIChE J 1972;18:670. [CrossRef]

[5] Sattar AM, Alam MM. Thermal diffusion as well as transpiration effects on MHD free convection and mass transfer flow past an accelerated vertical porous plate. Indian J Pure Appl Math 1994;25:679–688.

[6] Chamkha AJ, Rashad AM. Unsteady heat and mass transfer by MHD mixed convection flow from a rotating vertical cone with chemical reaction and Soret and Dufour effects. Can J Chem Eng 2014;92:758–767. [CrossRef]

[7] Mortimer RG, Eyring H. Elementary transition state theory of the Soret and Dufour effects. Proc Natl Acad Sci U S A 1980;77:1728–1731. [CrossRef]

[8] Tak S, Sunder Mathur R, Gehlot R, Kumar, Khan A. MHD free convection-radiation interaction along a vertical surface embedded in Darcian porous medium in presence of Soret and Dufour's effects. Therm Sci 2010;14:137–145. [CrossRef]

[9] Ahmed N, Sengupta S. Thermo-diffusion and diffusion-thermo effects on a three dimensional MHD mixed convection flow past an infinite vertical porous plate with thermal radiation. Magnetohydrodynamics 2011;47:41–60. [CrossRef]

[10] Moorthy MBK, Senthilvadivu K. Soret and Dufour effects on natural convection flow past a vertical surface in a porous medium with variable viscosity. J Appl Math 2012;2012:1–15. [CrossRef]

[11] Reddy PS, Chamkha AJ. Soret and Dufour effects on MHD convective flow of Al2O3-water and TiO2-water nanofluids past a stretching sheet in porous media with heat generation/absorption. Adv Powder Technol 2016;27:1207–1218. [CrossRef]

[12] Jha BK, Gambo YY. Soret and Dufour effects on transient free convention heat and mass transfer flow in a vertical channel with ramped wall temperature and specie concentration: an analytical approach. Arab J Basic Appl Sci 2020;27:344–357. [CrossRef]

[13] Bilal Ashraf M, Hayat T, Alsaedi A, Shehzad SA. Soret and Dufour effects on the mixed convection flow of an Oldroyd-B fluid with convective boundary conditions. Results Phys 2016;6:917–924. [CrossRef]

[14] Gbadeyan JA, Idowu AS, Ogunsola AW, Agboola OO, Olanrewaju PO. Heat and mass transfer for

Soret and Dufour's effect on mixed convection boundary layer flow over a stretching vertical surface in a porous medium filled with a viscoelastic fluid in the presence of magnetic field. Glob J Sci Frontier Res A Phys Space Sci 2011;11:97–114.

[15] Srinivasacharya D, Chetteti Ramreddy. Soret and Dufour Effects on Mixed Convection from an Exponentially Stretching Surface. Int J Nonlinear Sci 2011;12:60–68.

[16] Siddique I, Nadeem M, Awrejcewicz J, Pawłowski W. Soret and Dufour effects on unsteady MHD second-grade nanofluid flow across an exponentially stretching surface. Sci Rep 2022;12:11811. [CrossRef]

[17] Mahdy A. Soret and Dufour effect on double diffusion mixed convection from a vertical surface in a porous medium saturated with a non-Newtonian fluid. J Non-Newtonian Fluid Mech 2010;165:568–575. [CrossRef]

[18] Srinivasacharya D, RamReddy C. Cross-diffusion effects on mixed convection from an exponentially stretching surface in non-Darcy porous medium. Heat Transfer Asian Res 2013;42:111–124. [CrossRef]

[19] Shateyi S, Motsa SS, Sibanda P. The effects of thermal radiation, Hall currents, Soret, and Dufour on MHD flow by mixed convection over a vertical surface in porous media. Math Probl Eng 2010;2010:1–20. [CrossRef]

[20] Shaheen N, Alshehri HM, Ramzan M, Shah Z, Kumam P. Soret and Dufour effects on a Casson nanofluid flow past a deformable cylinder with variable characteristics and Arrhenius activation energy. Sci Rep 2021;11:19282. [CrossRef]

[21] Quader A, Alam MM. Soret and Dufour effects on unsteady free convection fluid flow in the presence of hall current and heat flux. J Appl Math Phys 2021;9:1611–1638. [CrossRef]

[22] Subhakar MJ, Gangadhar K, Reddy NB. Soret and Dufour effects on MHD convective flow of heat and mass transfer over a moving non-isothermal vertical plate with heat generation/absorption. Adv Appl Sci Res 2012;3:3165–3184.

[23] Balla CS, Ramesh A, Kishan N, Rashad AM. Impact of Soret and Dufour on bioconvective flow of nanofluid in porous square cavity. Heat Transfer 2021;50:5123–5147. [CrossRef]

[24] Siva Kumar Reddy B, Surya Narayana Rao KV, Vijaya RB. Soret and Dufour effects on MHD flow of viscoelastic fluid past an infinite vertical stretching sheet. Heat Transfer 2020;49:2330–2343. [CrossRef]

[25] Rashed GMA. Variable viscosity and thermophoresis for Soret and Dufour's effects on MHD generation in a non-Daracian porosity fluid. Heat Transfer 2020;49:1444–1457. [CrossRef]

[26] Sheikholeslami M, Gerdroodbary MB, Shafee A, Tlili I. Hybrid nanoparticles dispersion into water inside a porous wavy tank involving magnetic force. J Therm Anal Calorim 2019;141:1993–1999. [CrossRef]

[27] Manh TD, Bahramkhoo M, Barzegar Gerdroodbary MB, Nam ND, Tlili I. Investigation of nanomaterial flow through non-parallel plates. J Therm Anal Calorim 2020;143:3867–3875. [CrossRef]

[28] Manh TD, Abazari AM, Barzegar Gerdroodbary MB, Nam ND, Moradi R, Babazadeh H. Computational simulation of variable magnetic force on heat characteristics of backward-facing step flow. J Therm Anal Calorim 2020;144:1585–1596. [CrossRef]

[29] Tlili I, Moradi R, Barzegar Gerdroodbary MB. Transient nanofluid squeezing cooling process using aluminum oxide nanoparticle. Int J Mod Phys C 2019;30:1950078. [CrossRef]

[30] Barzegar Gerdroodbary MB. Application of neural network on heat transfer enhancement of magneto-hydrodynamic nanofluid. Heat Transfer Asian Res 2019;49:197–212. [CrossRef]

[31] Man Y, Gerdroodbary MB. Influence of Lorentz forces on forced convection of nanofluid in a porous enclosure. J Porous Media 2024;27:15–25. [CrossRef]

[32] Barzegar Gerdroodbary MB, Jafaryar M, Sheikholeslami M, Amini Y. The efficacy of magnetic force on thermal performance of ferrofluid in a screw tube. Case Stud Therm Eng 2023;49:103187. [CrossRef]

[33] Kumar KA, Sugunamma V, Sandeep N. Thermophoresis and Brownian motion effects on MHD micropolar nanofluid flow past a stretching surface with non-uniform heat source/sink. Comput Therm Sci An Int J 2020;12:55–77. [CrossRef]

[34] Roja P, Sankar Reddy T, Ibrahim SM, Lorenzini G, Sidik NAC. The effect of thermophoresis on MHD stream of a micropolar liquid through a porous medium with variable heat and mass flux and thermal radiation. CFD Lett 2022;14:118–136. [CrossRef]

[35] Zaman SU, Nauman Aslam M, Hussain A. Chemically reactive MHD fluid flow along with thermophoresis and Brownian effects. Adv Mech Eng 2023;15:16878132231193326. [CrossRef]

[36] Sidahmed AOM, Department of Mathematics, College of Science and Arts, King Abdulaziz University, Rabigh 21911, Saudi Arabia. Numerical solution for MHD flow of an Oldroyd–B fluid over a stretching sheet in the presence of thermophoresis with chemical reaction effects. Int J Adv Appl Sci 2023;10:121–131. [CrossRef]

[37] Hussain Z, Ayaz M, Islam S. Effects of thermophoresis and Brownian motion on radiative MHD hybrid nanofluid flow over a stretching sheet with convective boundary conditions: A homotopic approach. Proc Inst Mech Eng Part N J Nanomater Nanoeng Nanosyst 2024;23977914231225019. [CrossRef]

[38] Chintalapudi R, Koti H, Shashidar Reddy B, Saritha K. Mechanisms of diffusion thermo and thermal diffusion on MHD mixed convection flow of Casson fluid over a vertical cone with porous material in the

presence of thermophoresis and Brownian motion. J Adv Res Numer Heat Transf 2024;17:29–43. [CrossRef]
[39] Sarma AK, Sarma D. MHD flow in free convection over an exponentially stretched sheet submerged in a double-stratified medium. Int J Ambient Energy 2024;45:1. [CrossRef]
[40] Sarma AK. Unsteady radiative MHD flow over a porous stretching plate. In: Modeling and Simulation of Fluid Flow and Heat Transfer. 2024:96–109. [CrossRef]
[41] Choudhary K, Jha AK, Mishra LN, Vandana Ms. Buoyancy and chemical reaction effects on MHD free convective slip flow of Newtonian and polar fluid through porous medium in the presence of thermal radiation and ohmic heating with Dufour effect. Facta Univ, Ser Math Informatics 2018;33:1. [CrossRef]
[42] Sharma N, Mishra LN, Mishra VN. Fixed point theorems for expansive type mappings in multiplicative metric spaces. Turkish J Anal Numer Theory 2018;6:52–56.
[43] Bhat IA, Mishra LN, Mishra VN, Tunç C, Tunç O. Precision and efficiency of an interpolation approach to weakly singular integral equations. Int J Numer Methods Heat Fluid Flow 2024;34:1479–1499. [CrossRef]
[44] Rathour L, Singh V, Yadav H, Sharma MK, Mishra VN. A dual hesitant fuzzy set theoretic approach in fuzzy reliability analysis of a fuzzy system. Inf Sci Lett 2024;13:433–440. [CrossRef]
[45] Sharma MK, Chaudhary S, Rathour L, Mishra VN. Modified genetic algorithm with novel crossover and mutation operator in traveling salesman problem. Sigma J Eng Nat Sci 2024;42:6. [CrossRef]
[46] Negero NT, Duressa GF, Rathour L, Mishra VN. A novel fitted numerical scheme for singularly perturbed delay parabolic problems with two small parameters. Partial Differ Equ Appl Math 2023;8:100546. [CrossRef]
[47] Hogeme MS, Woldaregay MM, Rathour L, Mishra VN. A stable numerical method for singularly perturbed Fredholm integro differential equation using exponentially fitted difference method. J Comput Appl Math 2024;441:115709. [CrossRef]
[48] Sheikholeslami M, Kataria HR, Mittal AS. Effect of thermal diffusion and heat generation on MHD nanofluid flow past an oscillating vertical plate through porous medium. J Mol Liq 2018;257:12–25. [CrossRef]
[49] Kataria HR, Mittal AS. Velocity, mass and temperature analysis of gravity-driven convection nanofluid flow past an oscillating vertical plate in the presence of magnetic field in a porous medium. Appl Therm Eng 2017;110:864–874. [CrossRef]
[50] Kataria HR, Mittal AS. Mathematical model for velocity and temperature of gravity-driven convective optically thick nanofluid flow past an oscillating vertical plate in presence of magnetic field and radiation. J Niger Math Soc 2015;34:303–317. [CrossRef]
[51] Sheikholeslami M, Kataria HR, Mittal AS. Radiation effects on heat transfer of three dimensional nanofluid flow considering thermal interfacial resistance and micro mixing in suspensions. Chin J Phys 2017;55:2254–2272. [CrossRef]
[52] Li Z, Sheikholeslami M, Mittal AS, Shafee A, Haq RU. Nanofluid heat transfer in a porous duct in the presence of Lorentz forces using the lattice Boltzmann method. Eur Phys J Plus 2019;134:1. [CrossRef]
[53] Patel HR, Mittal AS, Darji RR. MHD flow of micropolar nanofluid over a stretching/shrinking sheet considering radiation. Int Commun Heat Mass Transf 2019;108:104322. [CrossRef]
[54] Mittal AS, Patel HR. Influence of thermophoresis and Brownian motion on mixed convection two dimensional MHD Casson fluid flow with non-linear radiation and heat generation. Physica A 2020;537:122710. [CrossRef]
[55] Kataria HR, Mittal AS. Analysis of Casson nanofluid flow in presence of magnetic field and radiation. Math Today 2017;33:99–120.
[56] Mittal AS, Kataria HR. Three dimensional CuO–Water nanofluid flow considering Brownian motion in presence of radiation. Karbala Int J Mod Sci 2018;4:275–286. [CrossRef]
[57] Kataria HR, Mittal AS. Mathematical analysis of three dimensional nanofluid flow in a rotating system considering thermal interfacial resistance and Brownian motion in suspensions through porous medium. Math Today 2018;34:A:7–24.
[58] Mittal AS, Patel HR, Darji RR. Mixed convection micropolar ferrofluid flow with viscous dissipation, Joule heating and convective boundary conditions. Int Commun Heat Mass Transf 2019;108:104320. [CrossRef]
[59] Mittal AS. Analysis of water-based composite MHD fluid flow using HAM. Int J Ambient Energy 2021;42:1538–1550. [CrossRef]
[60] Mittal AS. Study of radiation effects on unsteady 2D MHD Al2O3-water flow through parallel squeezing plates. Int J Ambient Energy 2022;43:653–660. [CrossRef]
[61] Kataria HR, Mistry M, Mittal A. Influence of nonlinear radiation on MHD micropolar fluid flow with viscous dissipation. Heat Transfer 2022;51:1449–1467. [CrossRef]
[62] Kataria H, Mittal AS, Mistry M. Effect of nonlinear radiation on entropy optimised MHD fluid flow. Int J Ambient Energy 2022;43:6909–6918. [CrossRef]
[63] Palani S. A comparative exploration of a magnetized power-law fluid past an inclined plate with variable physical properties. Sigma J Eng Nat Sci 2024;1:72. [CrossRef]

[64] El Hattab M. MHD natural convection in a square enclosure using carbon nanotube-water nanofluid with two isothermal fins. Sigma J Eng Nat Sci 2024;1:87. [CrossRef]

[65] Kumar Sarma A. MHD flow and effects of Hall current, Joule heating, and heat source across a chemically reacting and radiating exponentially stretching sheet in a porous medium. Sigma J Eng Nat Sci 2024;1:110. [CrossRef]

[66] Ishak A. Unsteady MHD flow and heat transfer over a stretching plate. J Appl Sci 2010;10:2127–2131. [CrossRef]

[67] Shampine LF, Kierzenka J, Reichelt MW. Solving boundary value problems for ordinary differential equations in MATLAB with bvp4c. Tutorial notes 2000;1–27.

[68] Mwamba N, Okelo Abonyo J, Awuor KO. Effects of thermal radiation and chemical reaction on hydromagnetic fluid flow in a cylindrical collapsible tube with an obstacle. Int J Math Math Sci 2023;2023:1–15. [CrossRef]

[69] Elbashbeshy EMA, Aldawody DA. Heat transfer over an unsteady stretching surface with variable heat flux in the presence of a heat source or sink. Comput Math Appl 2010;60:2806–2811. [CrossRef]